Catalysis Letters (2020) 150:95–105
https://doi.org/10.1007/s10562-019-02955-9

A Facile Synthesis of Pd–C_3N_4@Titanate Nanotube Catalyst: Highly Efficient in Mizoroki–Heck, Suzuki–Miyaura C–C Couplings

Venkata Ramana Kumar Velpula[1,2] · Thirupathaiah Ketike[1] · Gidyonu Paleti[1,2] · Seetha Rama Rao Kamaraju[1,2] · David Raju Burri[1,2]

Received: 19 June 2019 / Accepted: 4 September 2019 / Published online: 13 September 2019

Abstract

A Pd–C_3N_4@titanate nanotube (Pd–C_3N_4@TNT) catalyst workable in water medium, robust against leaching and agglomeration was prepared in a facile synthetic procedure using quite common chemicals such as TiO_2 powder, urea and palladium acetate. The Pd–C_3N_4@TNT catalyst has been characterized by BET surface area and pore size distribution, X-ray diffraction, solid-state ^{13}C NMR spectroscopy, X-ray photoelectron spectroscopy and transmission electron microscopy. The Pd–C_3N_4@TNT is a green catalyst for the Miziroki–Heck and Suzuki–Miyaura C–C coupling reactions in water medium with high efficiency (˃ 99% product yields) due to atomic level immobilization of Pd in C_3N_4 networked titanate nanotubes. Pd–C_3N_4@TNT is robust against leaching and agglomeration due to stable and furthermore it is recyclable and usable at least for five repeated cycles. The use of water as solvent, absence of leaching and agglomeration, recyclability and reusability ascertains the greenness of Pd–C_3N_4@TNT) catalyst and process.

Electronic supplementary material The online version of this article (https://doi.org/10.1007/s10562-019-02955-9) contains supplementary material, which is available to authorized users.

✉ David Raju Burri
david.iict@gov.in

[1] Catalysis & Fine Chemicals Department, CSIR-Indian Institute of Chemical Technology, Hyderabad 500007, India

[2] CSIR-Academy of Scientific and Innovative Research (CSIR-AcSIR), New Delhi, India

Graphic Abstract

Novel Pd–C_3N_4@titanate nanotube catalyst prepared from bulk TiO_2 and urea by simple hydrothermal and thermal pyrolysis followed by immobilization of Pd is active and selective for Mizoroki–Heck, Suzuki–Miyaura C–C couplings in water medium.

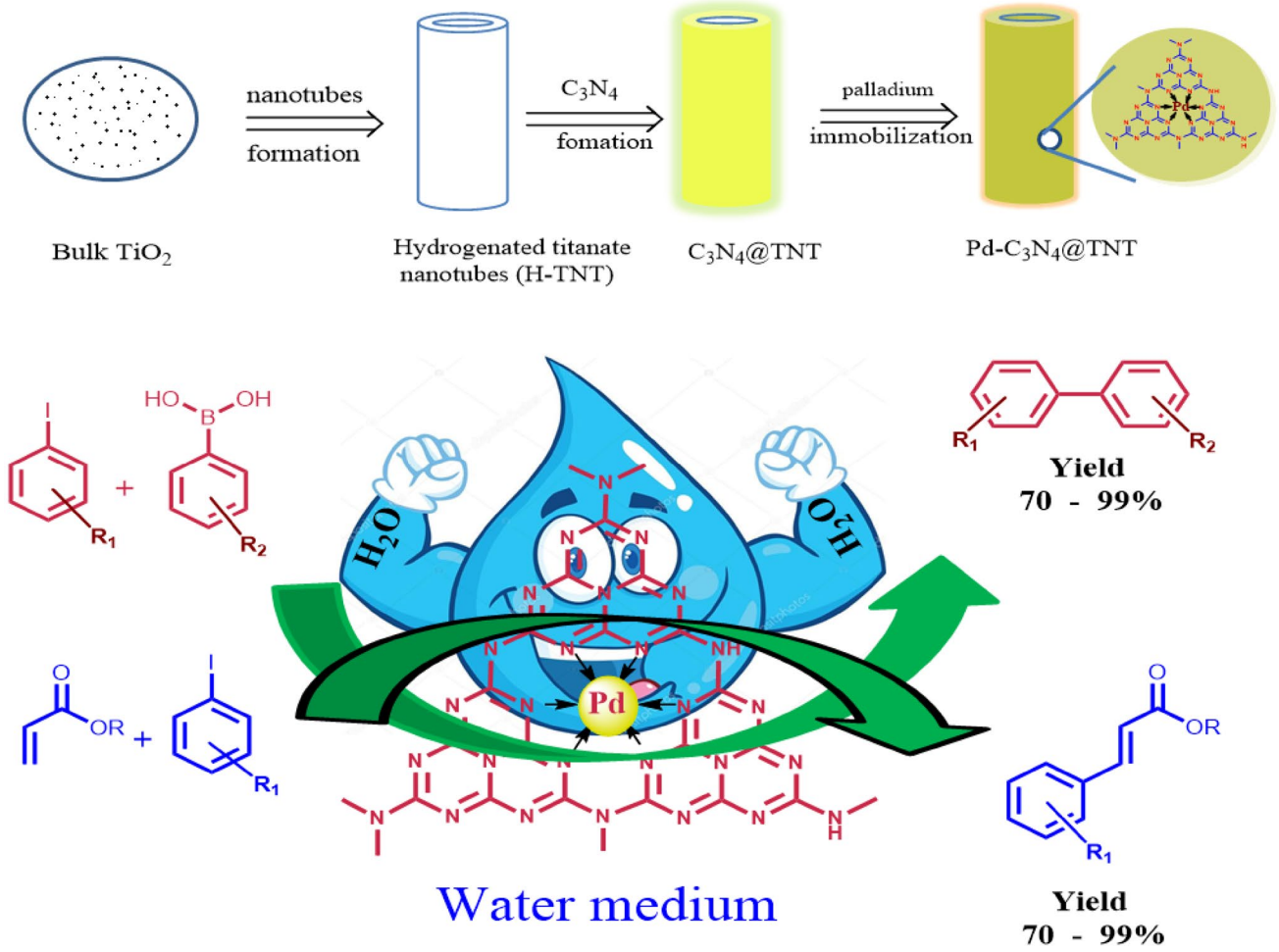

Keywords Titanate nanotube · C–C coupling · Pd · C_3N_4

Abbreviations

TNT	Titanate nanotubes
H-TNT	Hydrogenated titanate nanotubes
GVL	Gamma-Valerolactone
DCM	Dichloromethane
GC	Gas chromatography
GC-MS	Chromatography–mass spectrometry

1 Introduction

Noble metals are capable of catalyzing most of the organic transformations [1–3], wherein, palladium is one of the key transition metals, generally engaged as an efficient catalyst for the cross-coupling reactions of Mizoroki–Heck and Suzuki–Miyaura reactions, which are the most promising synthetic routes in pharmaceutical industries. Most of these industries rely on homogeneous Pd catalysts, but the involvement of difficulties in catalyst separation and its reusability are unavoidable. Palladium contamination in the product is also one of the notable issues. To overcome these difficulties the research directed towards the development of heterogeneous catalysts. Unambiguously, the problem of catalyst separation and recyclability was solved with heterogeneous catalysts, but the leaching and agglomeration of palladium [4–7] are the most unwanted issues still to be resolved. Phosphine ligands are being used to stabilize Pd species, prevention of Pd agglomeration followed by inactive palladium

black formation [8, 9]. Product contamination with ligand residues is one of the notable issues in pharmaceutical industries. The permissible limit of contamination is generally below 10 ppm [10], hence developments of alternative eco-friendly heterogeneous catalysts are highly desirable. To circumvent the problem of palladium leaching, different porous materials having peculiar porous network were used as supports, which are capable of preventing the leaching by accommodate palladium particle in the pore texture. But, still complete prevention of palladium leaching is not yet been achieved. In this context, immobilization of palladium with certain functional groups that are anchored to supports like silica, carbon, polymer, Pd@CDNS–g–C_3N_4, ordered mesoporous SBA-15/$PrSO_3$ and metal–organic framework [11–18] is one of the important options.

Supports having high surface area, suitable porosity, held with organic functional groups capable of firm anchoring of palladium are highly desirable to prevent the leaching. Hydrogen titanate nanotubes are intensively studied materials, attracting much attention in the past decade due to unique textural and physicochemical properties including versatile applications, particularly in catalysis and photo catalysis. Titanate nanotubes that are synthesized from TiO_2 nanoparticles (particle size < 25 nm) by hydrothermal method possess high specific surface area (≈ 200–400 m^2/g), which are widely used because of their flexibility towards desired modifications. Albeit, the preparation of titanate nanotubes from TiO_2 nanoparticles well established, preparing from commercial TiO_2 powder are limited.

Amine and imine functional groups are the most common chelating agents which are anchored to the surface of the catalyst supports. Polydopamine (PDA) deposition on the silicone nanofilament is one of the best known example [19].The suppression ofPd leaching by nitrogen and oxygen containing polymer is exploited in nitrogen rich triazine functionalized mesoporous covalent organic polymer [20].

According to earlier reports TiO_2 and SiO_2 were modified with urea and termed as N-doping or N-modification, but the actual N-species has not been identified. The subsequent studies revealed that the N-doped species is C_3N_4 on the surface of TiO_2 powder using the surface –OH of bulk TiO_2. It can be ascertain that it is not only a simple nitrogen insertion but also surface modification with triazine ring derivatives (malon) [21]. Pyrolysis of urea beyond 400°C gives graphitic carbon nitride [22], similarly, pyrolysis of urea in presence of titania and silica at 350–400°C produces a unique materials of (C_3N_4 triazine) derivatives covalently attached to the semiconductor which is also called as covalently coupled inorganic–organic semiconductor [23].

The commonly used solvents for Miziroki–Heck and Suzuki–Miyaura C–C coupling are dimethylformamide, dimethylsulfoxide, N-methylpyrrolidin-2-one and N,N-dimethylacetamide. Of late, attention is diverted towards non-toxic bio-mass derived renewable solvent like γ-Valerolactone [24]. But less attention is being paid to use water as a solvent even though it is cheap, abundant and clean.

The present work deals with the design and synthesis of novel heterogeneous palladium catalyst (Pd–C_3N_4@TNT) for effective utilization in Mizoroki–Heck and Suzuki–Miyaura carbon–carbon bond forming reactions under eco-friendly water medium. To the best of our knowledge synthesis of melon (C_3N_4) anchored titanium nanotubes (TNT), immobilization of palladium in melon network to attain atomic level dispersion of palladium, maintain the leaching-free, agglomeration-free environment, application as catalyst for Mizoroki–Heck and Suzuki–Miyaura carbon–carbon bond forming reactions under eco-friendly water medium is the first report. Herein, details of catalyst preparation, characterization and catalytic applications are delineated.

2 Experimental Section

2.1 Synthesis of Pd–C_3N_4@TNT Catalyst and Catalytic Activity

Synthesis of catalyst involves (i) the transformation of bulk TiO_2 powder into titanate nanotubes (ii) initial formation of sodium form of titanate nanotubes, (iii) transformation of sodium form of titanate nanotubes (Na-TNT) into H form of titanate nanotubes (H-TNT), (iv) anchoring of C_3N_4 (melon) to H-TNT, and (v) immobilization of palladium in the C_3N_4 network. The detailed catalyst synthesis is as follows.

2.2 Synthesis of H-TNT

Typically, 2.5 g of commercially available TiO_2 (Sigma–Aldrich) powder was dispersed in 10 M NaOH (200 ml) aqueous solution and subjected to hydrothermal treatment at 130 °C in a Teflon-lined autoclave (250 ml capacity) for 48 h under autogeneous pressure in static condition. After cooling to room temperature, precipitate was separated by filtration and washed thoroughly with distilled water. The resultant white precipitate is the sodium form of titanate nanotubes (Na-TNT), which was treated with 0.1 M HCl (1000 ml) at room temperature under constant stirring for 12 h, filtered, washed, dried at 100 °C for 12 h, which results the formation of H form titanate nanotubes, hereafter this material is used as H-TNT [25].

2.3 Anchoring of C_3N_4 to H-TNT

Anchoring of C_3N_4 to H-TNT was achieved by pyrolysis of urea. In a typical procedure, 1 g of HTNT was

dispersed in 50 ml of aqueous urea solution (5 g urea in 50 ml of water) stirred at RT for 1 h and evaporated the excess water on a water bath, dried at 60°C for 6 h followed by hot air oven at 100 °C for 12 h. The resultant material was taken in a glass reactor in between the two layers of glass wool. On the top layer of glass wool 5 g of urea was placed and increased the temperature to 400 °C in the flow of N_2 gas and calcined at 400°C for 2 h in N_2 gas environment (inert atmosphere). The obtained yellow materials was washed with water (200 ml) and ethanol (50 ml) and dried at 100°C in a hot air oven for 12 h, yielded the graphitic-C_3N_4 anchored to H-TNT, which is hereafter presented as C_3N_4@TNT.

The proposed mechanism of C_3N_4 formation and its anchoring on TNT was displayed in Scheme 1. As per previously reported in literature [21, 23] the thermal pyrolysis of urea to melamine which give to polymerized to C_3N_4 lead in four steps (1) urea decomposition to isocyanic acid (2) the reacts with isocyanic acid forms Ti–NH_2 and CO_2 (3) some of isocyanic acid convert to its tautomer cyanic acid (4) cyanic acid reacts with Ti–NH_2 gives cyanamide. It is necessary to presence of OH groups containing a catalyst to convert cyanamide, which can trimerize to melamine, in the absence of the heterogeneous catalyst, melamine is formed only under high-pressure conditions. Calcination environment is a crucial step to get C_3N_4@TNT. Unless N_2 atmosphere is maintained the resultant product is N-doped TiO_2 nanotubes (N-TNT) which is confirmed by ^{13}C NMR.

2.4 Immobilization of Palladium

0.975 g of C_3N_4@TNT was dispersed in 30 ml of DCM and sonicated for 30 min. 0.053 g of palladium acetate dissolved in 50 ml of DCM was slowly added to the sonicated C_3N_4@TNT under content stirring at room temperature for 3 h, centrifuged and the obtained solid material was kept in oven for drying at 100°C for 12 h, followed by annealing at 250 °C for 1 h under N_2 flow. The resultant palladium immobilized C_3N_4@TNT is coded as Pd–C_3N_4@TNT, where the palladium loading is around 2 wt% determined by SEM–EDX analysis Fig. 1.

3 Results and Discussion

The elemental mapping of Pd–C_3N_4@TNT was made and the images are presented in Fig. 2, which shows that the spacial arrangement of C, N, Pd, Ti, and O respectively and are homogeneously distributed.

Surface area and pore volume of H-TNT, C_3N_4@TNT and Pd–C_3N_4@TNT are listed in Table 1, gradual decrease in surface area and pore volume from H-TNT to C_3N_4@TNT confirming the anchoring of C_3N_4 onto H-TNT. Since surface area and pore volume of C_3N_4@TNT and Pd–C_3N_4@TNT are more or less equal, immobilization of palladium within C_3N_4 networked titanate nanotubes can be ascertained. The amount of Pd in Pd–C_3N_4@TNT was measured by ICP-OES and it is 1.7 wt%.

TEM images were shown in Fig. 3, convey the titanate nanotubes produced from titanium powder retained their

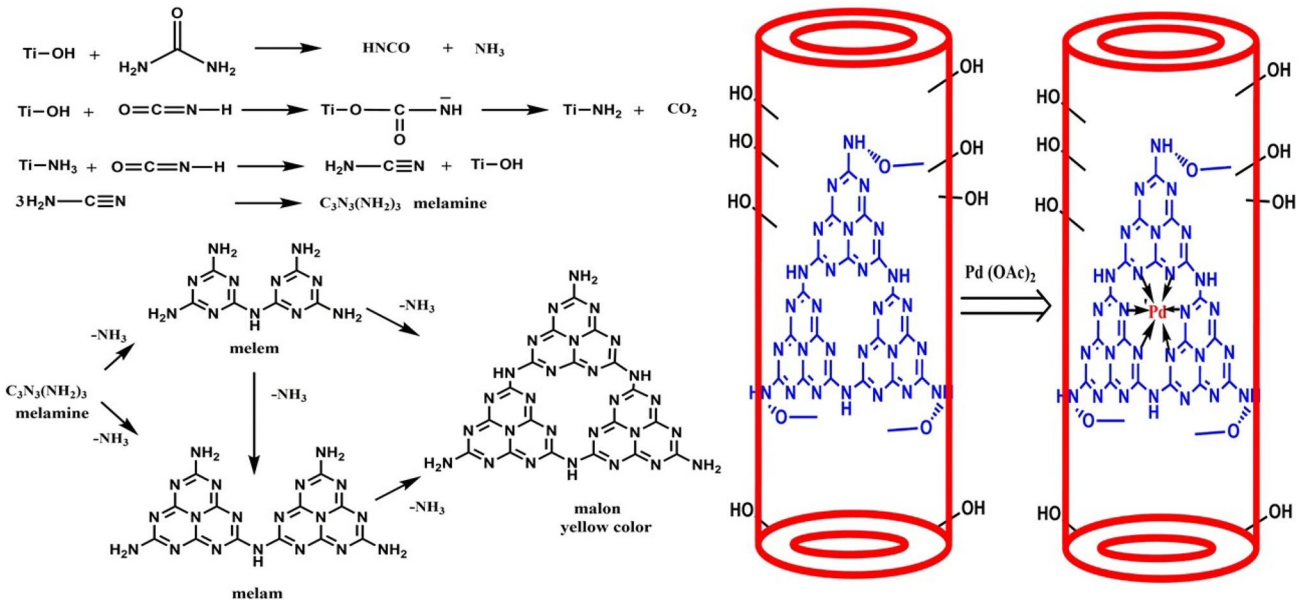

Scheme 1 Schematic representation of C_3N_4@TNT synthesis

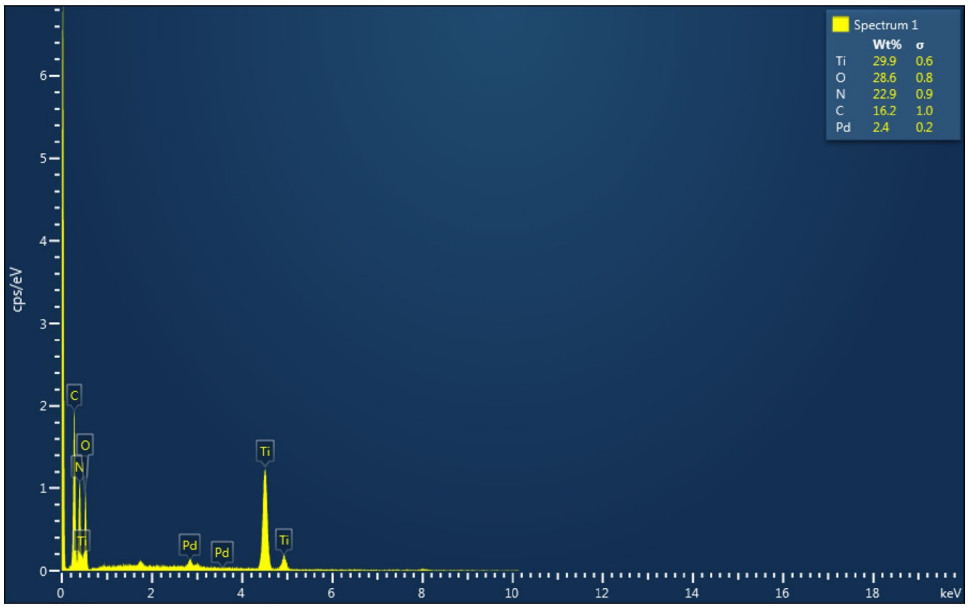

Fig. 1 SEM-EDX of Pd–C_3N_4@TNT

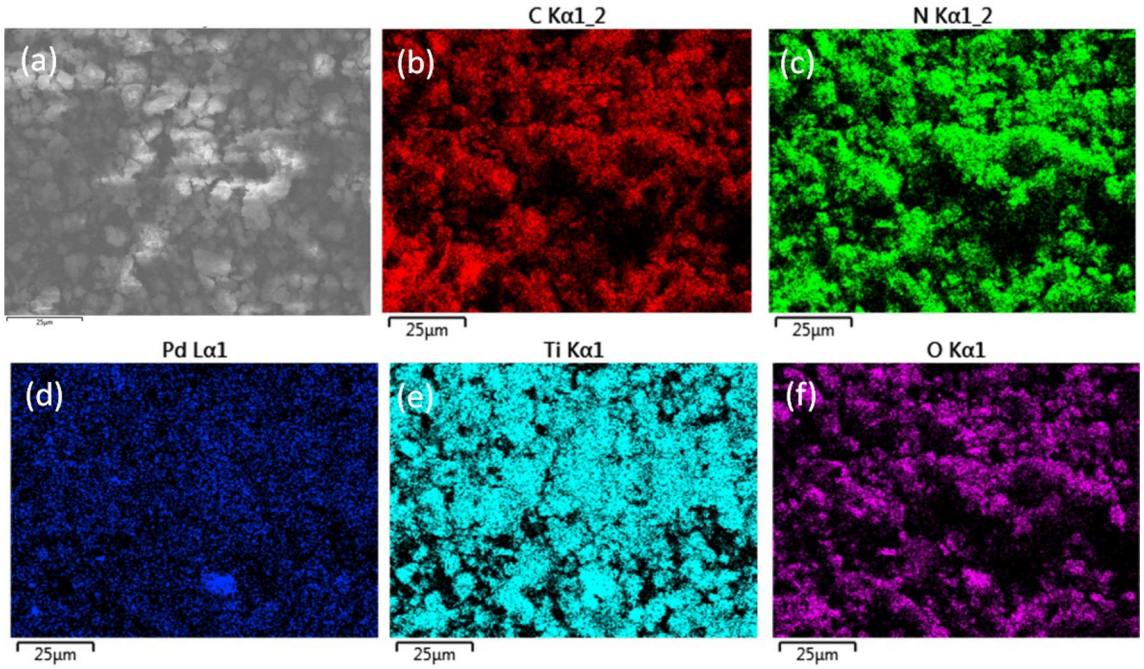

Fig. 2 **a** SEM image of Pd–C_3N_4@TNT the resultant color-coded Single-element distribution maps of Pd–C_3N_4@TNT containing, **b** C, **c** N, **d** Pd, **e** Ti, **f** O

Table 1 BET surface area of TNT catalysts

S. no	Sample	BET (m^2/g)
1	H-TNT	181
2	C_2N_4@TNT	114
3	Pd–C_2N_4@TNT	105

tubular structure with internal diameter 4.834 nm and interlayer distance of 0.35 nm even after the anchoring of C_3N_4 and the palladium immobilization From Fig. 4, the C_3N_4 formation has been confirmed using ^{13}C NMR spectroscopic analysis. Solid state ^{13}C NMR chemical shifts values for Pd–TNT@C_3N_4 obtained in the region of 163.86 ppm and

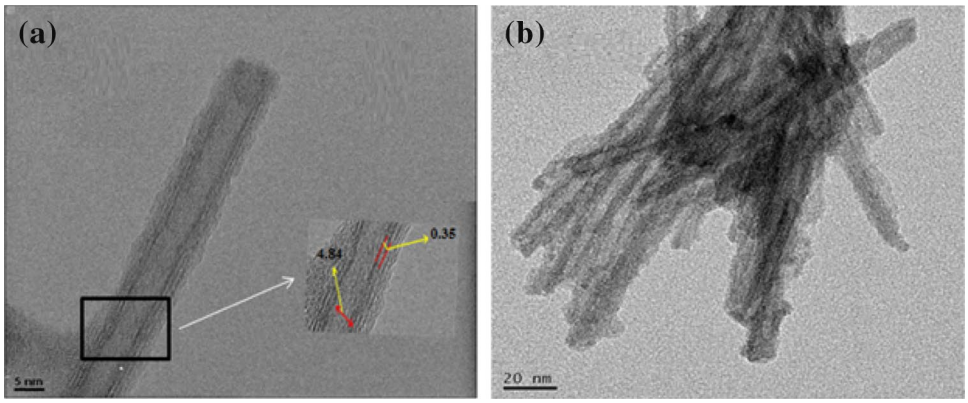

Fig. 3 TEM images **a** titanate nanotubes, **b** Pd–C_3N_4@TNT

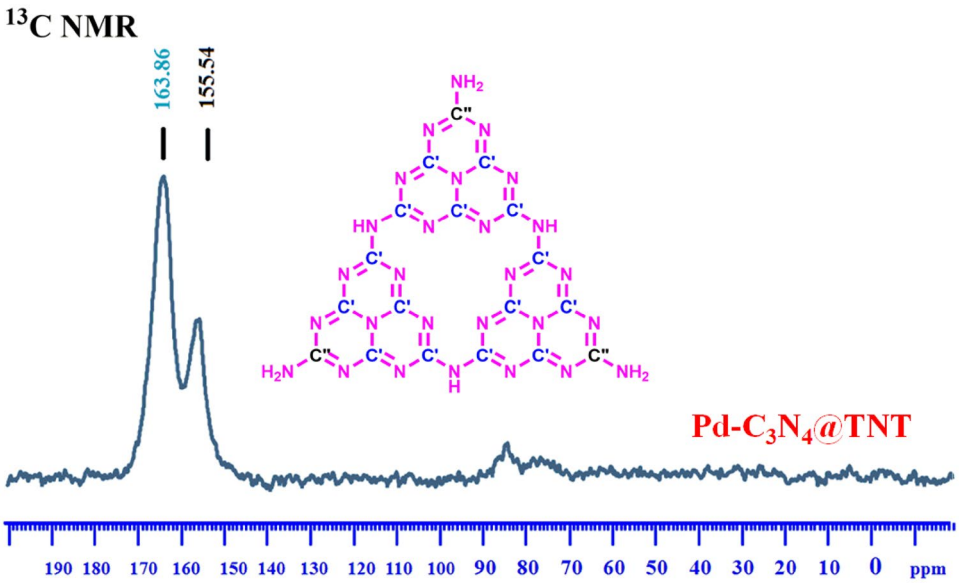

Fig. 4 Solid state ^{13}C NMR of C_3N_4@ TNT and N-TNT

155.54 ppm. The ^{13}C NMR spectral signals at 165 ppm and 155.1 ppm represent the poly(tri-s-triazine) structure which is the characteristic of carbon nitride [26–29].Close observation of ^{13}C spectral signals at 163.86 ppm and was assigned to C atoms that were not associated with sp^3 N, whereas a second peak at 155.54 ppm was suggested to represent C atoms close to the bridging –N groups rather than at 165 ppm and 155.1 revealing the interaction of C_3N_4 with titanate nanotubes as well as immobilized palladium species. It is one of the evidences for the formation of malon structure of graphitic carbon nitride (C_3N_4) and its interaction with both titanate nanotube and immobilized palladium. Similar observation was made by Gao et al. [30] when potassium was interacted with C_3N_4.

The XRD pattern of commercially purchased TiO_2 powder shown in Fig. 5 is in the anatase form in accordance with the diffraction peak positions at 2θ = 25.4, 37.9, 48.0, 54.0, 55.1,62.7, 68.8,70.4 and 75.1° and the corresponding (101), (004), (200), (105), (211), (204), (116), (200) and (215) crystal planes (JCPDS: 01-07-2486C). The XRD pattern

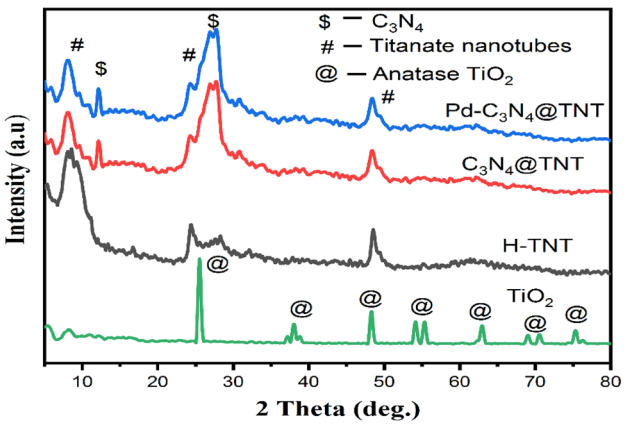

Fig. 5 XRD patterns of commercial TiO_2 powder, H-TNT, C_3N_4@ TNT and Pd–C_3N_4@TNT

of H-TNT is poorly resolved confirming the transformation of highly crystalline anatase TiO_2 into nanoscopic material (H-TNT). Albeit, the XRD pattern of H-TNT is poorly

crystalline, four diffraction peaks were observed at 2θ = 9.33, 24.1, 28.3, and 48.4°, which are typical of monoclinic layered hydrogen titanate (JCPDS-ICDD Card No. 47-0561). The diffractograms of C_3N_4@TNT and Pd–C_3N_4@TNT are similar to that of the diffractogram of H-TNT, except the appearance of XRD reflection at 2θ = 12.4° implying the distance between fragments of tri-s-triazine (C_3N_7) in (100) plane of graphitic–C_3N_4, (C_6N7)–N–(C_6N_7), the strongest peak at 27.6° (002) plane is a characteristic interplanar stacking peak of 2 aromatic systems.

According to X-ray photoelectron spectra (Fig. 6) the binding energies of carbon at 288.24 eV and N at 398.78 eV are responsible for sp^2 C=N bond in the g-C_3N_4 triazine ring and the peak for N at 400.99 assigned to $(C)_3$–N or $(C)_2$–N–H. The peaks at 288.24 eV and 284.6 eV in the C zone are attributed to electrons originating from a sp^2 carbon (C) atom attached to an NH_2 group and to an aromatic carbon atom [31, 32]. Whereas, the weak peak at 286.4 eV is ascribed to C–O from adsorbed CO_2 and absence of a peak at 290.7 eV indicating the complete consumption of urea [33]. The binding energies observed for both Pd–C_3N_4@TNT annealed catalyst (at 250°C) and used catalyst are at 343.0 eV, 337.8 eV and 341.0 eV, 335.8 eV respectively corresponding to Pd $3d_{3/2}$and Pd $3d_{5/2}$ indicating that metallic Pd and Pd^{2+} in both the catalysts Fig. 6d and e, confirming that both the catalysts reduced some extent during annealing and reaction, this phenomenon has been reported elsewhere. In Fig. 6c and f the shift in XPS spectra of titania 2p for H-TNT and C_3N_4@TNT were found at 459.29 and 464.6 eV of TiO_2 correspond to the Ti $2p_{3/2}$ and $2p_{1/2}$ respectively [34, 35].

In FT-IR spectra (Fig. 7) several bands are observed in the range of 1200–1650 cm^{-1} for C_3N_4@TNT, is characteristic of the usual stretching modes of C–N heterocycles. Another band found at 808 cm^{-1} is contributing from the ring sextant out-of-plane bending vibrations of triazine rings. The absence of a band at 2500 cm^{-1} indicating the absence of urea moiety, the broad bands at appears 3330 cm^{-1} and 3160 cm^{-1} are indicative of stretching vibration modes for OH and NH. These results further confirming that g-C_3N_4 structure in TNT prepared by the supramolecular aggregation from urea.

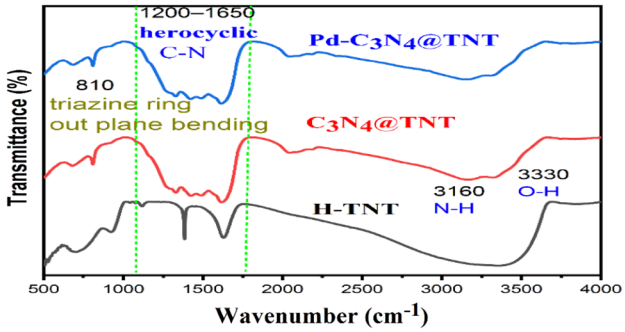

Fig. 7 FT-IR spectra of H-TNT, C_3N_4@TNT and Pd–C_3N_4@TNT

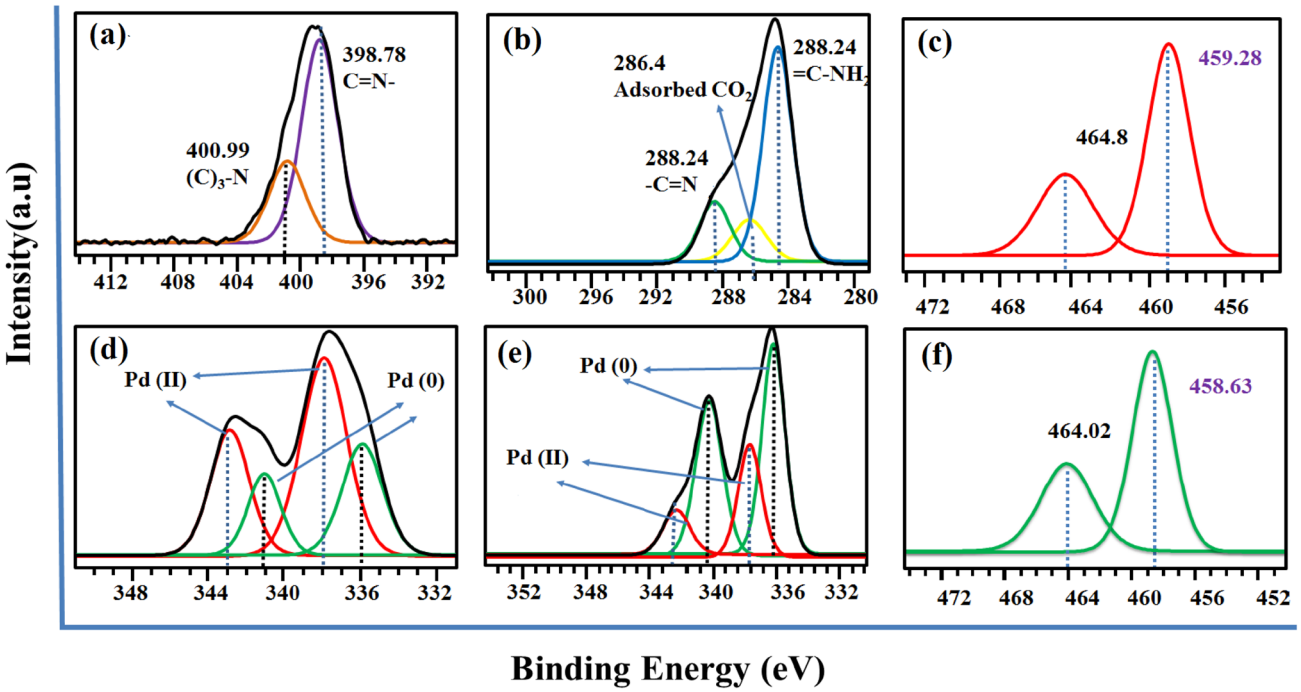

Fig. 6 XPS spectra of Pd–C_3N_4@TNT **a** N region, **b** C region, **c** Ti in H-TNT, **d** Pd in fresh catalyst, **e** Pd in used catalyst, **f** Ti in C_3N_4@TNT

3.1 Mizoroki–Heck Reaction

The catalytic activity of Pd–C_3N_4@TNT was determined in the liquid phase. In a typical procedure, 1 mmol acrylate 1 mmol iodobenzenes, 5 mol percent of TBAI, 10 mg of the Pd–C_3N_4@TNT catalyst and 3 ml of water were added to a RB flask and stirred magnetically at 75–80 °C in atmospheric conditions 45 min, the products were extracted with ethyl acetate and DCM mixture 3:1 the catalyst was separated by centrifugation. The catalytic activity of Pd–C_3N_4@TNT catalyst for the Mizoraki–Heck reaction was determined and data obtained at optimized conditions has been displayed in Table 2 and the scope of the catalyst performance has also been determined and the data displayed in Table 3. The TON and TOF of the Pd–C_3N_4@TNT catalyst for this reaction is 625 and 833 h^{-1} respectively.

3.2 Suzuki–Miyaura Coupling Reaction

The reaction was performed by taking 1.2 mmol of phenyl boronic acid, 1 mmol of iodobenzene, 1.5 mmol of Na_2CO_3 and 3 ml of water–ethanol (2:1 v/v) solvent at 80 °C for 1 h. The product mixture was extracted using ethyl acetate-dichloromethane (3:1, v/v) and analyzed by GC, prior to

Table 3 Scope of Mizoroki–Heck coupling over Pd–C_3N_4@TNT catalyst

Entry	R1	R2	Yield (%)
1	H	n-Butyl	≈ 99
2	4-Methyl	n-Butyl	93
3	2-Methoxy	n-Butyl	89
4	4-Methoxy	n-Butyl	≈ 99
5	4-Iodo	n-Butyl	71
6	2,4-Dimethoxy	n-Butyl	91
7	4-Amino	n-Butyl	83
8	H	Isobutyl	97
9	4-amino	Isobutyl	96
10	4-iodo	Isobutyl	65
11	2-methoxy	Isobutyl	70
12	4-methyl	Isobutyl	98
13	2,4-dimethoxy	Isobutyl	84
14	4-nitro	Isobutyl	65

Reaction conditions: butyl acrylate (1 mmol), aryl halide (1 mmol), and catalyst (10 mg), base (2 mmol), TBAI (tet-rabutyl ammonium iodide, 0.5 mmol) and solvent (2 ml)

Table 2 Optimization of reaction parameters over Pd–C_3N_4@TNT catalyst for Mizoroki–Heck coupling

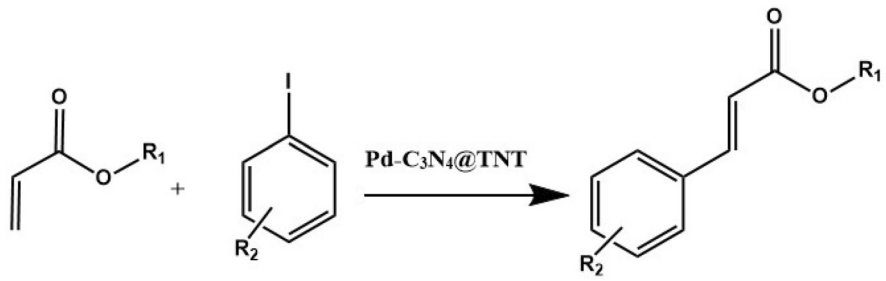

Entry	Solvent	Base	Temp. (°C)	Time (min)	Yield (%)
1	DMF	Et_3N	50	60	9
2	DMSO	Et_3N	50	60	Negligible
3	GVL	Et_3N	50	60	42.93
4	Water	Et_3N	50	60	45.6
5	ACN	Et_3N	50	60	19.5
6	Water	Et_3N	50	60	45
7	Water	Et_3N	65	60	94
8	Water	Et_3N	75	45	≈ 100
9	Water	K_2CO_3	75	45	44
10	Water	[a]DBU	75	45	53
11	Water	[b]NEDA	75	45	92

Reaction conditions: n-butyl acrylate (1 mmol), aryl halide (1 mmol), and catalyst (10 mg), base (2 mmol), TBAI (tetrabutyl ammonium iodide, 0.5 mmol) and solvent (2 ml), [a]DBU: 8-Diazabicyclo [5.4.0] undec-7-ene, [b]NEDA: N-ethyldiisopropylamine

Table 4 Scope of Suzuki–Miyaura coupling over Pd–C_3N_4@TNT catalyst

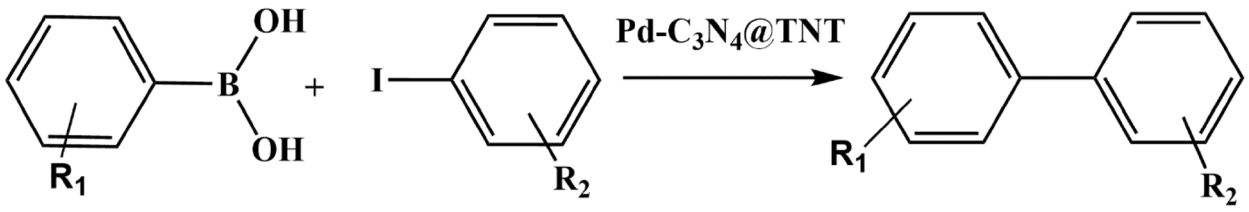

Entry	R_1	R_2	Yield (%)
1	H	H	≈ 100
2	H	4-Me	≈ 100
3	H	4-NO_2	≈ 100
4	H	4-NH_2	70
5	H	4-OMe	≈ 100
6	4-OMe	H	≈ 100
7	4-OMe	4-Me	≈ 100
8	4-OMe	4-NO_2	≈ 100
9	4-OMe	4-NH_2	≈ 100
10	4-OMe	4-OMe	≈ 100

Reaction conditions: 1.2 mmol of Aryl boronic acids, 1 mmol of aryl halide, 1.5 mmol of Na_2CO_3 and 3 ml of water–ethanol (2:1 v/v) solvent at 80 °C for 1 h

regular analysis the products were identified by GC–MS (Table 4).

3.3 Catalyst Reusability and Leaching Test

At the end of each cycle the catalyst was separated by centrifugation, washed with ethyl acetate-DCM (3:1, v/v) mixture and reused. Within 5 repeated cycles no significant loss in activity of Pd–C_3N_4@TNT catalyst was observed, revealing the robustness against agglomeration of active component, i.e., palladium species. Palladium leaching test was conducted by stopping the reaction at about half of the reaction time (after 30 min) and separated the catalyst from product mixture by centrifugation and continued the reaction for 3 h, but no change either in the conversion or in the product yield, confirming the absence of leached Pd in the product mixture. The product mixture was also analyzed by ICP-AES, no Pd species were observed. The spent Pd–C_3N_4@TNT catalyst was

Table 5 Comparison of catalytic performance of Pd–C_3N_4@TNT catalyst with reported catalytic systems

Catalyst	Reaction conditions	Yield (%)	Ref.
SBA–Pd° catalyst (10 mg, 0.157 mol%)	PEG (2 ml), and 3 mmol Na_2CO_3, at 100 °C, 20 min	91	[36]
poly (AAm–coHEMA)@TAP–POSS5@Pd–NPs	H_2O (2 ml), 2 mmol K_2CO_3, 100 °C, 5 h	96	[37]
ZrO_2@AEPH_2–PPh_2–Pd (0) (0.2 mol%)	PEG 600 (3 ml), 1.5 mmol K_2CO_3, at 100 °C, 20 min	95	[38]
Pd(0)–Arg–boehmite (2.7 mol%)	DMF, K_2CO_3, 120 °C, 50 min	98	[39]
Pd–pyridyl complexes films	DMF (6 ml), 2 mmol Na_2CO_3, 140 °C, 24 h	98	[40]
(GA-FSNP@Pd) (0.47 mol% Pd)	DMF:H_2O (2:1 ml), 110 °C, 30 min	90	[41]
IRMOF-3–Pd	DMA (0.5 ml), iodobenzene (0.2 mmol), methyl acrylate (0.3 mmol), base (0.3 mmol), Hexamethylenediamine, 140 °C, 15 min	100	[42]
SMNPs-DF–Pd	Solvent free, DABCO (1.5 mmol), 140 °C, 2 h	92	[43]
Pd$(OAc)_2$@SBA–15/PrEn	DMF:H_2O (2 ml),Et_3N 2 mmol, 80 °C, 1 h	97	[44]
Pd–C_3N_4@TNT	Base (2 mmol), TBAI (tetrabutyl ammonium iodide, 0.5 mmol) and solvent (2 ml), 45 min	~ 99	Present work

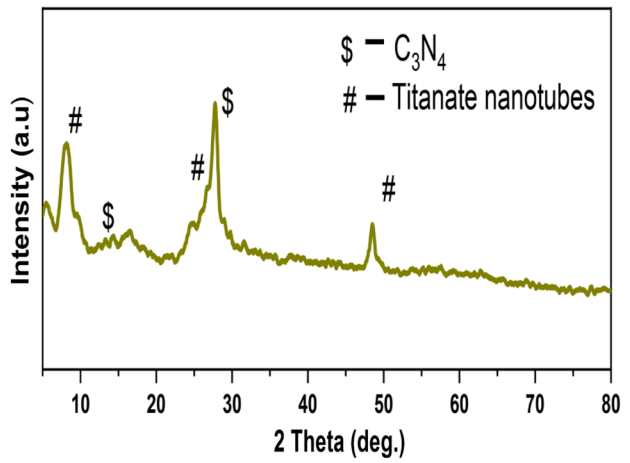

Fig. 8 XRD patterns of spent Pd–C_3N_4@TNT

also characterized by powder XRD and found that there is no significant structural change was observed. These results reveal that the Pd–C_3N_4@TNT is heterogeneous in nature. The high stability (neither leach nor agglomerate) of Pd–C_3N_4@TNT catalyst is due to reasons (i) Pd immobilization in the C_3N_4 network (ii) firm anchoring of C_3N_4 to TNT through elimination of water molecule from Ti–OH and –NH_2 group of C_3N_4 via Ti–NH bonding. As it is a solid catalyst ease of separation. High efficiency of Pd–C_3N_4@TNT is mainly due to isolated Pd species (Table 5, Fig. 8).

Activity point of view the present catalyst (Pd–C_3N_4@TNT) is the best catalyst, where as in the case of reference 37, 100% yield was claimed. In this particular work the amount of reactants taken are much lower and also carried out at high temperatures using organic solvent (DMA).

4 Conclusion

A novel palladium immobilized titanate nanotube (Pd–C_3N_4@TNT) catalyst was synthesized. The performance of this heterogeneous catalyst towards Mizoraki–Heck and Suzuki–Miyaura carbon–carbon bond forming reaction is on par with the reported superior catalysts and in addition this catalyst can be operated in water medium. The high performance of this catalyst may be due to atomic level Pd immobilization in the titanate nanotubes. Undeniably, this catalyst is robust against leaching and agglomeration, contributing the green chemistry.

Acknowledgements The author VVRK thanks Council of Scientific Industrial Research (CSIR), New Delhi, India for award of Fellowship. Manuscript Communication Number: IICT/Pubs./2019/215.

References

1. Lewis LN (1993) Chem Rev 93:2693–2730
2. Roucoux A, Schulz J, Patin H (2002) Catalysts Chem Rev 102:3757–3778
3. Turner V, Golovko B, Vaughan OP, Abdulkin P, Berenguer-Murcia A, Tikhov MS, Johnson BF, Lambert RM (2008) Nature 454:981–983
4. Bennur TH, Ramani A, Bal R, Chanda BM, Sivasanker S (2002) Catal Commun 3:493–496
5. Zhao F, Bhanage BM, Shirai M, Arai M (2000) Chem Eur J 6:843–848
6. Zhao F, Murakami K, Shirai M, Arai M (2000) J Catal 194:479–483
7. Köhler K, Heidenreich RG, Krauter JGE, Pietsch J (2002) Chem Eur J 3:622–631
8. Tromp M, Sietsma JRA, van Bokhoven JA, van Strijdonck GPFRJ, van Haaren AMJ, van der Eerden PWN, van Leeuwen M, Koningsberger DC (2003) Chem Commun 128–129
9. Iwasawa T, Tokunaga M, Obora Y, Tsuji Y (2004) J Am Chem Soc 126:6554–6555
10. Crevoisier M, Barle EL, Flueckiger A, Dolan DG, Ovais M, Walsh A (2016) Pharm Dev Technol 1:52–56
11. Veisi H, Mirzaee N (2018) Appl Organomet Chem 32:e4067
12. Herzing AA, Kiely CJ, Carley AF, Landon P, Hutchings GJ (2008) Science 321:1331–1335
13. Joo SH, Park JY, Tsung CK, Yamada Y, Yang P, Somorjai GA (2008) Nat Mater 8:126–131
14. Molnar A (2011) Chem Rev 111:2251–2320
15. Wang GH, Hilgert J, Richter FH, Wang F, Bongard HJ, Spliethoff B, Weidenthaler C, Schuth F (2014) Nat Mater 13:293–300
16. Sadjadi S, Heravi MM, Malmir M (2018) Carbohydr Polym 186:25–34
17. Martínez-Klimov ME, Hernandez-Hipólito P, Klimova TE, Solís-Casados DA, Martínez-García M (2016) J Catal 342:138–150
18. Jeong U, Teng X, Wang Y, Yang H, Xia Y (2007) Adv Mater 19:33–60
19. Fei X, Kong W, Chen X, Jiang X, Shao Z, Lee JY (2017) ACS Catal 7:2412–2418
20. Puthiaraj P, Pitchumani K (2014) Green Chem 16:4223–4233
21. Mitoraj D, Kisch H (2008) Angew Chem Int Ed 47:9975–9978
22. Liu J, Zhang T, Wang Z, Dawson G, Chen W (2011) J Mater Chem 21:14398
23. Mitoraj D, Kisch H (2010) Chem Eur J 16:261–269
24. Strappaveccia G, Ismalaj E, Petrucci C, Lanari D, Marrocchi A, Drees M, Facchetti A, Vaccaro L (2015) Green Chem 17:365–372
25. Niu L, Shao M, Wang S, Lu L, Gao H, Wang J (2008) J Mater Sci 43:1510–1514
26. Holst JR, Gillan EG (2008) J Am Chem Soc 13:7373–7379
27. Kailasam K, Epping JD, Thomas A, Losse S, Junge H (2011) Energy Environ Sci 4:4668–4674
28. Sun J, Zhang J, Zhang M, Antonietti M, Fu X, Wang X (2012) Nat Commun 3:1139
29. Makowski SJ, Kostler P, Schnick W (2012) Chem Eur J 18:3248–3257
30. Gao H, Yan S, Wang J, Zou Z (2014) Dalton Trans 43:8178
31. Homas TA, Fischer A, Goettmann F, Antonietti MJ, Muller O, Schloglb R, Carlssonc JM (2008) J Mater Chem 18:4893
32. Cui YJ, Ding Z, Fu X, Wang XC (2012) Angew Chem 124:11984
33. Zhu B, Xia P, Ho W, Yu J (2015) Appl Surf Sci 344:188–195
34. de Vries JG (2006) Dalton Trans 421
35. Köhler K, Heidenreich RG, Krauter JGE, Pietsch J (2002) Chem Eur J 8:622
36. Choghamarani AG, Derakhshan AA, Hajjami M, Rajabi L (2017) Catal Lett 147:110–127

37. Arsalani N, Akbari A, Amini M, Jabbari E, Gautam S, Chae KH (2017) Catal Lett 147:1086–1094
38. Razavi N, Akhlaghinia B, Jahanshahi R (2017) Catal Lett 147:360
39. Tahmasbi B, Ghorbani-Choghamarani A (2017) Catal Lett 147:649
40. Zhao X, Zhang J, Zhao Y, Li X (2015) Catal Lett 145:2010–2019
41. Tanhaei M, Mahjoub A, Nejat R (2018) Catal Lett 148:1549–1561
42. Nuri A, Vucetic N, Smått JH, Mansoori Y, Mikkola JP, Murzin YD (2019) Catal Lett 149:1941–1951
43. Zolfigol MA, Azadbakht T, Khakyzadeh V, Nejatyami R, Perrin D (2014) RSC Adv 4:40036
44. Rostamnia S, Liu X, Zheng D (2014) J Colloid Interface Sci 86–91